



**HAL**  
open science

## Partitioning between the inorganic chlorine reservoirs HCl and ClONO<sub>2</sub> during the Arctic winter 2005 from the ACE-FTS

G. Dufour, R. Nassar, C. D. Boone, R. Skelton, K. A. Walker, P. F. Bernath,  
C. P. Rinsland, K. Semeniuk, J. J. Jin, J. C. McConnell, et al.

► **To cite this version:**

G. Dufour, R. Nassar, C. D. Boone, R. Skelton, K. A. Walker, et al.. Partitioning between the inorganic chlorine reservoirs HCl and ClONO<sub>2</sub> during the Arctic winter 2005 from the ACE-FTS. *Atmospheric Chemistry and Physics*, 2006, 6 (8), pp.2355-2366. 10.5194/acp-6-2355-2006 . hal-00295951

**HAL Id: hal-00295951**

**<https://hal.science/hal-00295951>**

Submitted on 18 Jun 2008

**HAL** is a multi-disciplinary open access archive for the deposit and dissemination of scientific research documents, whether they are published or not. The documents may come from teaching and research institutions in France or abroad, or from public or private research centers.

L'archive ouverte pluridisciplinaire **HAL**, est destinée au dépôt et à la diffusion de documents scientifiques de niveau recherche, publiés ou non, émanant des établissements d'enseignement et de recherche français ou étrangers, des laboratoires publics ou privés.



Distributed under a Creative Commons Attribution 4.0 International License

# Partitioning between the inorganic chlorine reservoirs HCl and ClONO<sub>2</sub> during the Arctic winter 2005 from the ACE-FTS

G. Dufour<sup>1,\*</sup>, R. Nassar<sup>1</sup>, C. D. Boone<sup>1</sup>, R. Skelton<sup>1</sup>, K. A. Walker<sup>1</sup>, P. F. Bernath<sup>1</sup>, C. P. Rinsland<sup>2</sup>, K. Semeniuk<sup>3</sup>, J. J. Jin<sup>3</sup>, J. C. McConnell<sup>3</sup>, and G. L. Manney<sup>4,5</sup>

<sup>1</sup>Department of Chemistry, University of Waterloo, Ontario, Canada

<sup>2</sup>NASA Langley Research Center, Hampton, Virginia, USA

<sup>3</sup>Department of Space Science and Engineering, York University, Ontario, Canada

<sup>4</sup>NASA Jet Propulsion Laboratory/California Institute of Technology, Pasadena, California, USA

<sup>5</sup>New Mexico Institute of Mining and Technology, Socorro, New Mexico, USA

\* now at: Laboratoire de Météorologie Dynamique/Institut Pierre Simon Laplace, Palaiseau, France

Received: 4 November 2005 – Published in Atmos. Chem. Phys. Discuss.: 15 February 2006

Revised: 3 May 2006 – Accepted: 18 May 2006 – Published: 29 June 2006

**Abstract.** From January to March 2005, the Atmospheric Chemistry Experiment high resolution Fourier transform spectrometer (ACE-FTS) on SCISAT-1 measured many of the changes occurring in the Arctic (50–80° N) lower stratosphere under very cold winter conditions. Here we focus on the partitioning between the inorganic chlorine reservoirs HCl and ClONO<sub>2</sub> and their activation into ClO. The simultaneous measurement of these species by the ACE-FTS provides the data needed to follow chlorine activation during the Arctic winter and the recovery of the Cl-reservoir species ClONO<sub>2</sub> and HCl. The time evolution of HCl, ClONO<sub>2</sub> and ClO as well as the partitioning between the two reservoir molecules agrees well with previous observations and with our current understanding of chlorine activation during Arctic winter. The results of a chemical box model are also compared with the ACE-FTS measurements and are generally consistent with the measurements.

by heterogeneous reactions into active chlorine molecules (ClO<sub>x</sub>=ClO+2Cl<sub>2</sub>O<sub>2</sub>+2Cl<sub>2</sub>) that drive catalytic ozone destruction. In the Arctic, the peak of the ClO volume mixing ratio profile is at about 20–21 km and the chlorine activation typically extends up to ~25 km (Santee et al., 2003). In the presence of gaseous nitric acid (which allows the formation of NO<sub>x</sub> from the photolysis of HNO<sub>3</sub> and also from the reaction with OH) and modest levels of ozone (which allows the formation of ClO via Cl+O<sub>3</sub>), typical of the Arctic, ClO<sub>x</sub> deactivation proceeds by the formation of ClONO<sub>2</sub> by the three body reaction of ClO and NO<sub>2</sub>. The reformation of HCl via the reaction of Cl and CH<sub>4</sub> is slower than the formation of ClONO<sub>2</sub>. The strong denitrification, or at least the lack of gaseous HNO<sub>3</sub>, and the lack of O<sub>3</sub> in the Antarctic prevents the rapid recovery of ClONO<sub>2</sub>. The buildup of HCl thus occurs later in the Arctic spring by the slow conversion of ClONO<sub>2</sub> into HCl (Douglass et al., 1995; Müller et al., 1994; Santee et al., 1996; Chipperfield et al., 1996).

## 1 Introduction

The key role of chlorine species in the depletion of ozone occurring during cold Arctic winters and under high chlorine loading is now well demonstrated (WMO, 2003). A schematic description of the winter conversion of chlorine reservoir molecules to photochemically active species and of the subsequent reformation of the reservoir species in the spring is given by Michelsen et al. (1999, Plate 8). When the temperatures are sufficiently low to allow the formation of polar stratospheric clouds (PSCs), the chlorine reservoir species HCl and ClONO<sub>2</sub> are transformed

The time evolution of inorganic chlorine species during the polar winter and the early spring and their partitioning have been studied in both hemispheres from ground-based (Solomon et al., 2000; Mellqvist et al., 2002), airborne (Webster et al., 1993), balloon-borne (Payan et al., 1998; Stachnik et al., 1999), shuttle-borne (Rinsland et al., 1995; Michelsen et al., 1996), and satellite-borne (Dessler et al., 1995; Douglass et al., 1995; Santee et al., 1996; Höpfner et al., 2004) instruments. However, few instruments are able to measure HCl and ClONO<sub>2</sub> simultaneously. Ground-based FTIR spectrometers measure HCl and ClONO<sub>2</sub> columns continuously during winter and spring but sample one location (Blumenstock et al., 1997). Simultaneous vertical profiles of HCl and ClONO<sub>2</sub> have been reported (Payan et al., 1998; Stimpfle et al., 1999; Bonne et al., 2000) but for a limited time span and a

Correspondence to: G. Dufour  
(gaelle.dufour@lmd.polytechnique.fr)

**Table 1.** Error budget for HCl for a vortex occultation (sr7657)<sup>a</sup>.

Altitude km	vmr	Meas. noise	Spectr. Data <sup>b</sup>	Pointing <sup>c</sup>	T <sup>d</sup>	ILS <sup>e</sup>	Interferers <sup>f</sup>	Total error <sup>g</sup>
16.5	0.814	0.028	0.013	0.015	0.016	0.005	0.015	0.041 (5)
18.5	0.944	0.031	0.020	0.034	0.015	0.002	0.033	0.062 (7)
20.5	0.918	0.032	0.022	0.005	0.012	0.002	0.005	0.041 (4)
22.5	1.43	0.048	0.035	0.008	0.015	0.011	0.007	0.063 (4)
24.5	2.15	0.059	0.047	0.043	0.027	0.030	0.043	0.105 (5)
26.5	2.44	0.078	0.053	0.064	0.027	0.04	0.064	0.139 (6)
28.5	2.52	0.082	0.039	0.079	0.038	0.065	0.08	0.163 (6)

<sup>a</sup> HCl vmr values and the errors are in ppbv.

<sup>b</sup> Based on spectroscopic uncertainty of 2% as given in the HITRAN 2004 database.

<sup>c</sup> Based on a tangent height uncertainty of 150 m.

<sup>d</sup> Based on a temperature uncertainty of 2 K.

<sup>e</sup> Since the ILS is parameterized, uncertainty in the ILS is induced by perturbing the field of view by 5%.

<sup>f</sup> H<sub>2</sub>O, based on early validation results (10%) (McHugh et al., 2005).

<sup>g</sup> Relative total error (%) is given in parentheses.

limited area. As far as we know, ACE-FTS is the first remote sounding instrument capable of measuring vertical profiles of HCl and ClONO<sub>2</sub> (and ClO) simultaneously, of sampling many locations within the vortex and of following the chemical evolution of various species during most of the winter and spring. The ACE-FTS is the first space-borne instrument capable of measuring HCl, ClONO<sub>2</sub>, and ClO simultaneously. We report on the time series of the two reservoir molecules during the 2004/2005 Arctic winter and their partitioning as well as the evolution of chlorine monoxide. We compare the results to previous observations and to the calculations from a chemical box model.

## 2 ACE-FTS measurements

The Atmospheric Chemistry Experiment (ACE), also known as SCISAT-1, was launched on 12 August 2003 into a circular 74° inclination low-earth orbit at 650 km. It has global coverage from approximately 85° N to 85° S with a majority of measurements over the Arctic and the Antarctic (Bernath et al., 2005). ACE makes solar occultation measurements and can observe up to 15 sunsets and 15 sunrises per day. The primary ACE instrument is a high resolution (0.02 cm<sup>-1</sup>) Fourier transform spectrometer (ACE-FTS) operating between 750 and 4400 cm<sup>-1</sup>. Vertical profiles of temperature, pressure and various atmospheric constituents are retrieved with a vertical resolution of 3–4 km from the ACE-FTS spectra recorded at a series of tangent heights using a global fit approach based on a Levenberg-Marquardt non-linear least squares method (Boone et al., 2005). The fitting routine does not impose any constraints based on a priori information. The results presented herein correspond to version 2.2 of the retrieval algorithm using the HITRAN 2004 linelist (Rothman et al., 2005). Molecular

absorption lines are fitted in selected microwindows to determine temperature and volume mixing ratio profiles. A set of microwindows is determined for each target species and is optimized to reduce the impact of interferers and to retrieve the vertical profile over the broadest possible altitude range. HCl is retrieved between 8 and 57 km from a set of 22 microwindows with a maximum width of 0.5 cm<sup>-1</sup> in the 2700–3000 cm<sup>-1</sup> spectral range. The main interferers are CH<sub>4</sub> and O<sub>3</sub> and they are retrieved simultaneously with the target species. H<sub>2</sub>O also contributes weakly and its volume mixing ratio (vmr) is fixed to values retrieved in a first step. McHugh et al. (2005) showed in an initial comparison using version 1.0 (using only 13 microwindows for HCl and a reduced altitude range) that ACE HCl abundances are 10 to 20% larger than those of HALOE. More recently, Froidevaux et al. (2006) have found that the MLS HCl values are within ~5% of the ACE values (version 2.1, a near-real-time version of version 2.2) in the stratosphere up to about 1 hPa. For ClONO<sub>2</sub>, two microwindows are used (779.85–780.45 cm<sup>-1</sup> and 1291.8–1293.4 cm<sup>-1</sup>) to retrieve the profile between 12 and 35 km. The main interferers, O<sub>3</sub>, HNO<sub>3</sub>, N<sub>2</sub>O, and CH<sub>4</sub> are also fitted simultaneously, including 3 additional microwindows (1104.78–1105.08 cm<sup>-1</sup>, 1202.61–1203.11 cm<sup>-1</sup>, and 1728.03–1728.53 cm<sup>-1</sup>) to constrain better the interferers. As for the HCl retrieval, H<sub>2</sub>O also has a weak contribution to the spectrum in the microwindows selected and is fixed to previously retrieved values. Only a very preliminary validation of ACE-FTS version 1.0 ClONO<sub>2</sub> has been made using ground-based FTS instruments (Mahieu et al., 2005). For the few cases of close co-incidence, the agreement between ACE-FTS and ground-based ClONO<sub>2</sub> columns is within a few percent. Finally, the ClO retrieval is carried out between 11 and 30 km using the 821 to 846 cm<sup>-1</sup> spectral window. This window is similar to the one used by Glatthor et al. (2004) to retrieve ClO from MIPAS spectra.

**Table 2.** Error budget for ClONO<sub>2</sub> for a vortex occultation (sr7657)<sup>a</sup>.

Altitude km	vmr	Meas. noise	Spectr. Data <sup>b</sup>	Pointing <sup>c</sup>	T <sup>d</sup>	ILS <sup>e</sup>	Interferers <sup>f</sup>	Total error <sup>g</sup>
16.5	357	56	18	22	15	17	17	69 (19)
18.5	528	51	26	22	8	14	14	66 (12)
20.5	762	27	38	32	48	28	28	84 (11)
22.5	1010	35	51	53	68	40	41	120 (12)
24.5	1240	31	62	66	65	32	33	124 (10)
26.5	1190	42	60	81	71	38	39	141 (12)
28.5	970	44	49	66	70	42	43	131 (13)

<sup>a</sup> ClONO<sub>2</sub> vmr values and the errors are in pptv.

<sup>b</sup> Based on spectroscopic uncertainty of 5%.

<sup>c</sup> Based on a tangent height uncertainty of 150 m.

<sup>d</sup> Based on a temperature uncertainty of 2 K.

<sup>e</sup> Since the ILS is parameterized, uncertainty in the ILS is induced by perturbing the field of view by 5%.

<sup>f</sup> H<sub>2</sub>O, based on early validation results (10%) (McHugh et al., 2005).

<sup>g</sup> Relative total error (%) is given in parentheses.

**Table 3.** Error budget for ClO for a vortex occultation (sr7657)<sup>a</sup>.

Altitude km	vmr	Meas. noise	Spectr. Data <sup>b</sup>	Pointing <sup>c</sup>	T <sup>d</sup>	ILS <sup>e</sup>	Interferers <sup>f</sup>	Total error <sup>g</sup>
18.5	426	434	79	52	9	2	3	444 (104)
19.5	876	452	117	65	29	11	17	473 (54)
20.5	1310	454	143	38	55	30	46	483 (37)
21.5	1080	569	116	70	49	26	41	588 (54)
22.5	572	569	54	102	38	23	40	583 (102)

<sup>a</sup> ClO vmr values and the errors are in pptv.

<sup>b</sup> Based on spectroscopic uncertainty of 15% as given in the HITRAN 2004 database.

<sup>c</sup> Based on a tangent height uncertainty of 150 m.

<sup>d</sup> Based on a temperature uncertainty of 2 K.

<sup>e</sup> Since the ILS is parameterized, uncertainty in the ILS is induced by perturbing the field of view by 5%.

<sup>f</sup> H<sub>2</sub>O (10%), CO<sub>2</sub> (1%), O<sub>3</sub> (5%).

<sup>g</sup> Relative total error (%) is given in parentheses.

CFC-11 and HCFC-22, which contribute to the spectrum in this spectral region, are simultaneously fitted with ClO.

A sensitivity study of the retrieval of these three species with respect to parameter uncertainties has been performed by perturbing each parameter by  $1\sigma$  of its assumed uncertainty for a vortex occultation. Error sources accounting for uncertainties in temperature, tangent altitude pointing, spectroscopic data, instrumental line shape (ILS), and mixing ratios of the main interfering species are considered. The effects of uncertainties in the baseline of the spectra, spectral shifts and molecules simultaneously retrieved are not included in this sensitivity study because these parameters are fitted and so their errors are included in the  $1\sigma$  statistical error (also called the measurement noise error). Results are summarized in Tables 1, 2, and 3 for HCl, ClONO<sub>2</sub> and ClO, respectively. For the altitude range of our study (15–30 km), the total error budget for HCl is about 5%, in agreement with

validation results (Froidevaux et al., 2006). ClONO<sub>2</sub> total error is about 11% in the altitude range of interest (19–25 km). ClO total error is about 35% at the maximum of the profile and is reliable from 19 to 22 km. The main contribution to the ClO error budget is measurement noise error. This is mainly due to ice contamination of the detector for this time period, reducing the signal-to-noise ratio in the ClO microwindow region. Averaging ClO profiles is recommended to reduce errors (see Sect. 4.4).

### 3 Synoptic view of the winter 2005 during the observation period

To describe the temperature conditions in the Arctic polar stratosphere we have used the National Center for Environmental Prediction/National Center for Atmospheric Research Reanalysis data (hereinafter “NCEP data”) (Kistler et

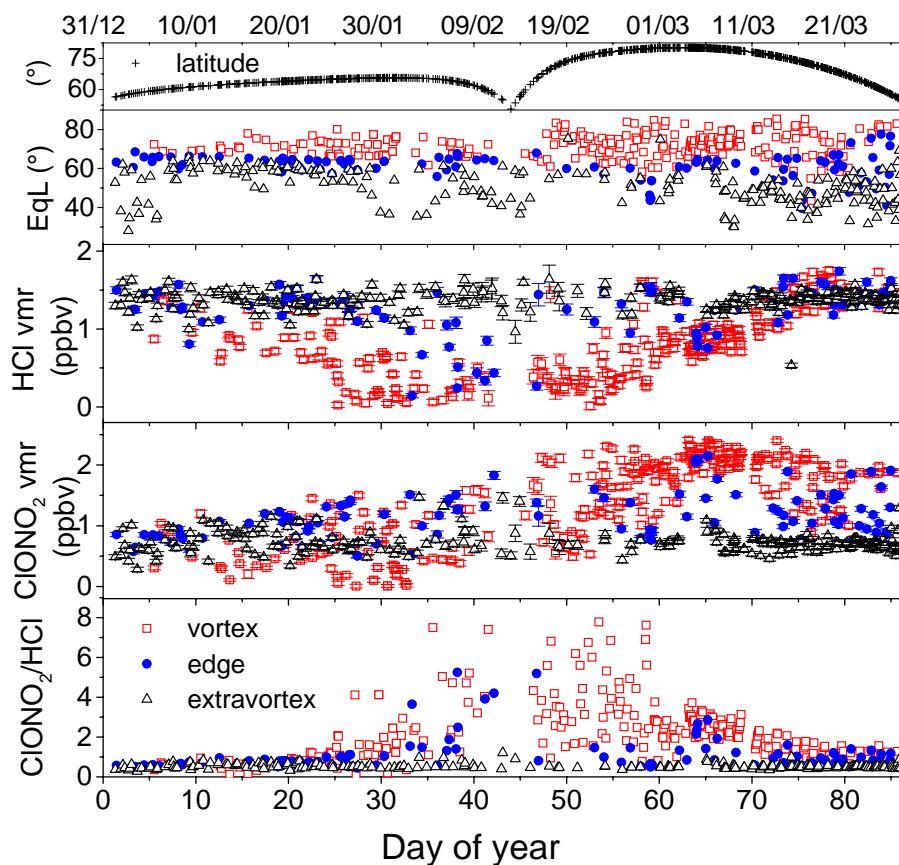


**Fig. 1.** Polar latitudes sounded by the ACE-FTS and the corresponding equivalent latitudes (upper panels) and time series of HCl, ClONO<sub>2</sub> and their ratio at 20.5 km (lower panels) during the Arctic winter 2005.

al., 2001). The region of interest for processing Cl<sub>y</sub> is largely from 70 hPa and 30 hPa. However, the lowest temperatures are found at 50 hPa (not shown) so we have described the evolution at this pressure level.

In mid-January, on the 50 hPa surface there is a cold pool with temperatures less than 191 K over northern Canada, poleward of 75° N which shifts eastward over Scandinavia and intensifies towards the end of the month. On 25 January the temperature minimum is less than 186 K at 77° N and 8° E. By early February the lowest temperatures, less than 189 K, are over Greenland and located at about 75° N. By 20 February the cold pool is found over the north Atlantic with the temperature minimum under 187 K. A strong warming occurs by the end of February and lasts into March so that temperatures conducive to polar stratospheric cloud formation are no longer present.

For most of January and February a significant region of the Arctic stratosphere has temperatures below 192 K and it is likely that nitric acid trihydrate (NAT) and supercooled ternary solution (STS) PSCs developed (e.g. Kleinböhl et al., 2005; Jin et al., private communication, 2005, have also seen denitrification using the ACE data). Given the observed wa-

ter vapor mixing ratios, it is likely that ice and STS PSCs form during late January and late February when temperatures fall below 187 K.

Any bias in the NCEP assimilated temperature data is likely to be towards higher values (Manney et al., 2003) so it is probable that temperatures even less than 186 K were present in early 2005. The spatial extent of the regions with temperatures low enough for PSC formation is sufficient for a significant portion of the vortex-confined air mass to experience heterogeneous chemical processing during its slow descent through the 50 hPa surface (e.g. Kleinböhl et al., 2005). It is likely that heterogeneous processing occurred in a larger volume of vortex air than indicated by the NCEP data.

#### 4 Results and discussion

For this study we focus on measurements obtained over the Arctic (from 50° N to 80° N) between 1 January 2005 and 26 March 2005. The upper panels of Fig. 1 show the latitudes sounded during the observation time period and the corresponding equivalent latitudes (the latitude that would enclose the same area between it and the pole as a given potential

vorticity (PV) contour) at 20.5 km. Each occultation was classified as inside, on the edge or outside the vortex, depending on the position of its reference latitude and longitude relative to the vortex edge. The classification method used here is a slightly modified version of the method described by Nassar et al. (2005). The occultations were classified based on the 15–25 km altitude range that includes the altitude of maximum chlorine activation and of the recovery near 20 km. The edge classification includes both occultations that truly cross the edge of the vortex, as well as those with a mixture of vortex and extravortex characteristics between 15 and 25 km due to the highly variable vortex of the 2005 Arctic winter. The results obtained were also verified by visual inspection of PV maps at 490 K ( $\sim 18$ – $19$  km) from GEOS-4 (Goddard Earth Observing System, Version 4.03) analyses (Bloom et al., 2005).

The three lowest panels of Fig. 1 show the time series of the volume mixing ratios (vmrs) of HCl and ClONO<sub>2</sub> and their ratio at 20.5 km from 1 January 2005 to 26 March 2005 for the occultations inside, on the edge and outside the vortex. For occultations defined as extravortex, the HCl vmr values at 20.5 km are about 1.5 ppbv while the ClONO<sub>2</sub> vmr values are about 0.75 ppbv, with a ClONO<sub>2</sub>/HCl ratio of about 0.5 (lowest panel). This ratio value is characteristic of unprocessed air masses and consistent with previous observations (Rinsland et al., 1995) although somewhat lower than that given by the box model (see below). In the case of occultations on the vortex edge, the trends of HCl, ClONO<sub>2</sub> and their ratio during the polar winter are more difficult to establish due to the smaller number of measurements near the vortex edge and the greater uncertainty in classification of measurements there. However, their behavior is generally quite similar to the behavior of occultations inside the vortex and the recovery of ClONO<sub>2</sub> seems to occur first on the edge as described by Chipperfield et al. (1997). It is worth noting that these results have to be interpreted carefully and may be due to a sampling issue as well as to uncertainty in the classification of an occultation as on the vortex edge. Furthermore, air masses sounded on the vortex edge may have also experienced less processing than some vortex measurements. On the contrary, in the case of vortex occultations, the large number of measurements permits us to follow all stages from chlorine activation to reservoir molecule recovery. However, it is worth noting that the sampling of air masses within the vortex is poor at the beginning of the observation period (Fig. 1, second panel) but increases during the winter and becomes rather good during the late winter and the early spring (reservoir recovery period). We also note that the occultations measured during most of February correspond to an observation period with very high beta angles ( $>55^\circ$  between 7 February and 21 February 2005). The beta angle is the angle between the orbital plane and the earth-sun vector. At high beta angles, the latitudes and longitudes sounded during an occultation vary significantly between the highest and the lowest tangent heights, and the

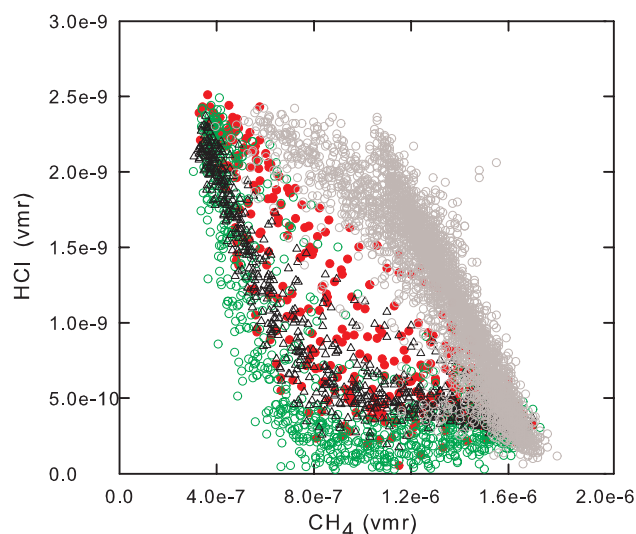


**Fig. 2.** Correlation plot of measured HCl versus measured CH<sub>4</sub> between 350 K and 700 K (approximately 12–26 km). Gray circles are observations outside the vortex at 3 January–26 March 2005; red dots are observations in the vortex for 1–25 January 2005; green circles are observations in the vortex for 26 January–25 February 2005; black are observations in the vortex for 26 February–24 March 2005.

number of measured spectra per occultation increases substantially, which leads to unstable retrievals. Relatively few profiles are available as shown in Fig. 1.

#### 4.1 Evolution of HCl inside the vortex

For HCl, the start of the decrease is observed at the beginning of January and becomes more pronounced after 20 January 2005 (Fig. 1). The minimum value of the HCl vmr ( $\sim 0.2$  ppbv) is reached around 25 January and low values persist until 25 February. After this period of very low levels of HCl, a slow recovery occurs from the end of February until the end of our measurement period, when HCl reaches values close to those characteristic of unprocessed air masses.

The correlation plot of HCl versus CH<sub>4</sub> between potential temperatures of 350 K and 700 K (approximately 12–26 km) in Fig. 2 shows another view of the evolution of HCl inside the vortex which also allows for descent. Gray circles, corresponding to measurements outside the vortex, are used as a reference for unprocessed air masses. Similar conclusions to those discussed for the level at 20.5 km can be drawn: from the variation it can be seen that HCl is processed progressively and sporadically throughout January. It is also clear from this figure that the HCl is quite variable throughout the vortex. The maximum of HCl processing occurs between 25 January and mid-February and this is followed by a slow recovery of HCl during March. We note that HCl is not completely recovered at the end of our measurement period inside

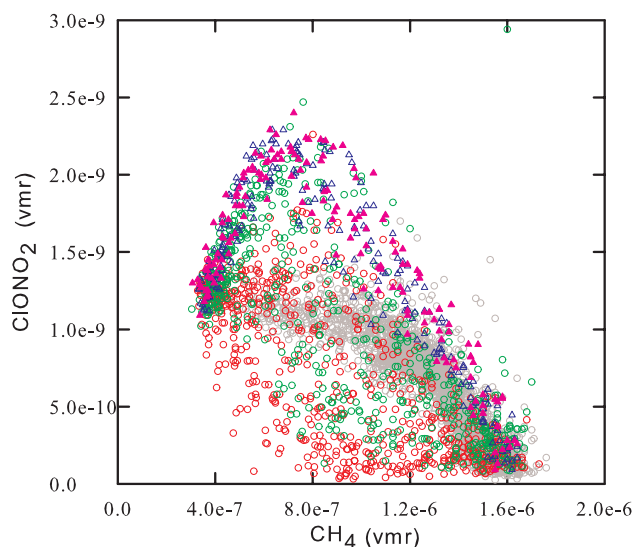


**Fig. 3.** Correlation plot of measured  $\text{ClONO}_2$  versus measured  $\text{CH}_4$  between 350 K and 700 K (approximately 12–26 km). Gray circles are observations outside the vortex for 1 January–26 March 2005; color symbols are observation in the vortex: red circles, 3 January–15 February 2005; green circles, 16–28 February 2005; blue triangles, 2–9 March 2005; purple triangles, 11–24 March 2005.

air masses remaining from vortex air (the vortex is breaking down during March).

#### 4.2 Evolution of $\text{ClONO}_2$ inside the vortex

In early January, the  $\text{ClONO}_2$  vmr in the vortex at 20.5 km is quite variable and the higher values suggest that some processing has already taken place (Fig. 1). From 20 to 30 January the  $\text{ClONO}_2$  varies from less than 0.1 ppbv to over 1.5 ppbv suggesting that the ACE-FTS is sampling air that has recently undergone processing so there has not been sufficient time to convert the ClO to  $\text{ClONO}_2$  while the higher values suggest that either the ClO resulting from earlier processing has been converted to  $\text{ClONO}_2$  (This is also suggested by the ClO plot in Fig. 4 which shows that the ClO has decreased during this period.) or the air masses sampled were not processed (due to the variability in the vortex position with respect to ACE observations).

The  $\text{ClONO}_2$  variability within the vortex is also clearly shown by the correlation of  $\text{ClONO}_2$  and  $\text{CH}_4$  in Fig. 3 for the period 1–25 January (red circles). From 18 February to the beginning of March  $\text{ClONO}_2$  is also quite variable. The lowest values are not as low as those in January and indicate less extensive processing or mixing of non-vortex air. We note that the  $\text{N}_2\text{O}-\text{CH}_4$  correlations inside and outside the vortex indicate that there has not been much mixing of non-vortex air during this period (Jin et al., 2006). However, it is worth pointing out that Manney et al. (2006) show evidence of mixing into and within the vortex throughout the winter,

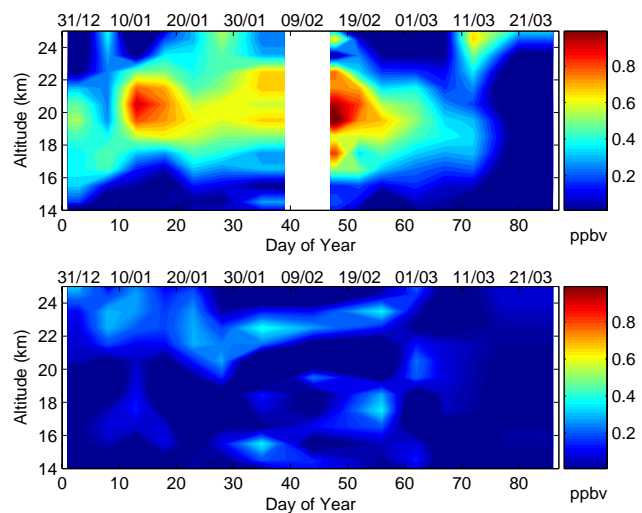


**Fig. 4.** Time series of average ClO profiles measured by ACE-FTS between 14 and 25 km during the Arctic winter of 2005. Upper panel: measurements corresponding to processed air masses. Lower panel: measurements corresponding to unprocessed air masses (see text for details).

and this gets stronger in late February. The higher values of  $\text{ClONO}_2$  (up to 2.2 ppbv), much larger than those typical of unprocessed air masses (gray circles in Fig. 3) suggest that the air parcels have been highly processed and the ClO converted back to  $\text{ClONO}_2$ .

At the 20.5 km level the maximum of  $\text{ClONO}_2$  vmr occurs between 2 and 10 March, with values between 2 and 2.5 ppbv, consistent with observations made by Payan et al. (1998) during March 1995. After 10 March,  $\text{ClONO}_2$  decreases as it is slowly converted into HCl. However, as evidenced from the correlation plot (Fig. 3)  $\text{ClONO}_2$  vmrs remain high until 24 March at other levels.

#### 4.3 Evolution of the inorganic chlorine partitioning

Concerning the partitioning between HCl and  $\text{ClONO}_2$ , their ratio ( $\text{ClONO}_2/\text{HCl}$ ) is about 0.5 on average (Fig. 1) during the first stage of chlorine activation (i.e., when both HCl and  $\text{ClONO}_2$  decrease). When HCl and  $\text{ClONO}_2$  are both at their lowest levels (25 January–3 February), the ratio increases and varies between 0 and 4 with a significant number of values higher than 1. During this time period,  $\text{ClONO}_2$  is, in general, higher than HCl because of its re-formation from ClO and  $\text{NO}_2$  from photolysis of  $\text{HNO}_3$  as noted above. The recovery begins after 4 February and the  $\text{ClONO}_2/\text{HCl}$  ratio reaches values as high as 8 between 18 and 28 February. As HCl begins to recover at the end of February, the ratio decreases progressively until 26 March. The ratio value is between 2.5 and 3 for the first 10 days of March as observed by Payan et al. (1998) during March 1995.

#### 4.4 Evolution of ClO inside the vortex

ClO profiles are also retrieved from ACE-FTS spectra. Due to ice contamination on the detector during the measurement period, individual profiles of ClO are not completely reliable and require averaging. We have done this in the following fashion. The occultations were divided into 2 groups in order to average profiles corresponding to similar air masses. Measurements within the vortex or on the edge were chosen based on HCl vmrs at 19.5 km and 20.5 km. If these values are lower than 1 ppbv, then the occultations can be averaged together. The reliability of this criterion was checked by averaging ClO profiles corresponding to HCl values higher than 1 ppbv at 19.5 and 20.5 km for periods of 5 days between 1 January and 26 March. The time series obtained is presented in the lower panel of Fig. 4. ClO vmrs are less than 0.4 ppbv and negligible for all altitudes, within one standard deviation.

We average ClO profiles with the following criteria: occultations have to be within 5 days and the difference in latitude should not exceed  $2^\circ$ . Profiles that have unphysical oscillations for the entire altitude range (11–30 km) are also rejected. This is particularly the case for occultations with beta angles higher than  $56^\circ$  (8–19 February). For this special case, only occultations after 15 February have realistic ClO profiles. The criterion based on latitude ( $2^\circ$ ) is relaxed and the ClO profiles between 15 and 19 February are averaged together. The upper panel of Fig. 4 shows the time series obtained. Sampling is an issue for the reliability of the averages. The average profiles between 20 January and 10 March are based on more than 10 individual profiles and are thus reliable. Outside this time period, the profiles just give the general trend of the time evolution of ClO. Although MLS data show that Cl-activation is significant by the end of December and quite substantial in the first 10 days of January (Santee et al., 2006<sup>1</sup>), the activation is apparent in the ACE data only from 10 January to the beginning of March. Note that PSCs are also observed in some ACE-FTS spectra during this time period (M. Eremenko, private communication). The occurrence of PSCs took place from 24 January to 2 February and from 17 February to 23 February, corresponding well with the observed ClO activation. The beginning of chlorine activation corresponds well to the decrease in HCl and ClONO<sub>2</sub> levels and the end of activation to the maximum recovery of ClONO<sub>2</sub> (2–10 March). Occultations before mid-February correspond to sunrise measurements and occultations after mid-February to sunset measurements. The amounts of ClO are then larger during sunsets than for sunrises when the dimer Cl<sub>2</sub>O<sub>2</sub> is still present in significant amounts. The maximum vmr value for ClO (about 1.07 ppbv) is reached near

20 km during the period of 15–19 February. This maximum value is smaller than the climatological values derived by Santee et al. (2003, Fig. 2) from MLS/UARS data recorded between 1991 and 1998. These values are between 1.20 and 1.35 ppbv for an equivalent latitude of  $74^\circ$  N (that corresponds to the mean equivalent latitude of ACE-FTS measurements inside the vortex for the time period 15–19 February). It is worth noting that only data with a solar zenith angle,  $\text{SZA} < 88^\circ$  (daylight) have been considered by Santee et al., while ACE-FTS data are given at  $90^\circ$  due to the measurement geometry. The ACE-FTS ClO vmrs are consequently smaller. The maximum ClO value derived from ACE-FTS measurements is also much smaller than values regularly observed in Antarctic ( $> 2$  ppbv) (Glatthor et al., 2004; Santee et al., 2003). The mean value of ClO during the activation period is about 0.6–0.7 ppbv corresponding to moderate activation.

## 5 Comparison with a chemical box model

Three-dimensional trajectories were produced using NCEP wind and temperature data. Multiple trajectories were initialized from the January and February ACE occultation locations at different altitudes and evolved for 60 days. Only trajectories that stay confined to the polar region are considered. Thus although this is not a domain-filling method it should, however, allow a reasonable representation of the type of processing that the ACE measurement locations should have encountered. It should also give a reasonable idea of the variation of species within the vortex, again as viewed by the ACE-FTS instrument. Of course, it is not expected that parcel identity can persist this long in reality, but these trajectories give an indication of the chemical environment present inside the vortex. Some fraction of vortex air will experience multiple heterogeneous chemical processing events while some fraction will not be affected by processing. Mixing will smear out the sharp differences between the air parcels found in the trajectory modeling.

The photochemical calculations have been done with a box model (Chartrand and McConnell, 1998) with updated rate data including heterogeneous chemistry on ice and STS polar stratospheric clouds. STS is assumed to grow on sulfate aerosols, which have a fixed climatological distribution. The STS parameterization is based on Carslaw et al. (1995). The STS surface area is related to the volume following the expression of Massie et al. (1998). Below the ice point the fraction of water vapour above the equilibrium vapor pressure (from the expression of Marti and Mauersberger, 1993), with a supersaturation ratio of 1.4, is assumed to form ice and the associated surface area is determined assuming a mean radius of 10 microns. PSCs in our model are determined at every time step based on ambient conditions but there is no tracking of particle growth or decay. A NAT parameterization is not included since it is felt that a good understanding

<sup>1</sup>Santee, M. L., MacKenzie, I. A., Manney, G. L., et al.: A study of stratospheric chlorine partitioning in the winter polar vortices based on new satellite measurements and modeling, in preparation, 2006.



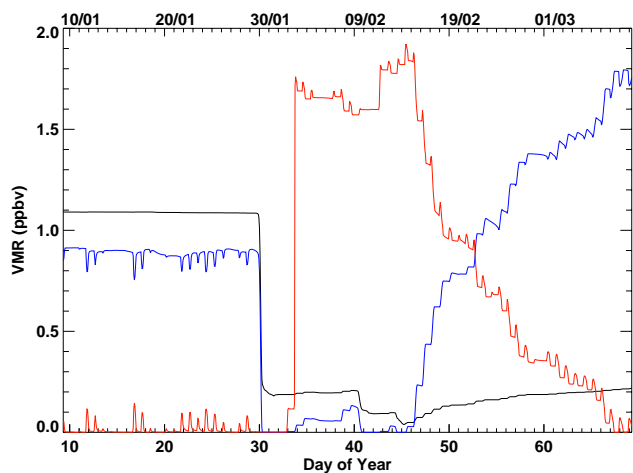


**Fig. 5.** HCl (black),  $\text{ClONO}_2$  (blue) and  $\text{ClO}_x$  (loosely defined as  $\text{ClO} + 2\text{Cl}_2\text{O}_2$ ) (red) vmrs for a 3-D trajectory launched from an ACE observation location ( $61.1^\circ\text{N}$ ,  $49.8^\circ\text{E}$ ) at 06:00 GMT on 9 January 2005 and followed out for 60 days, using NCEP data. For initial conditions see text.

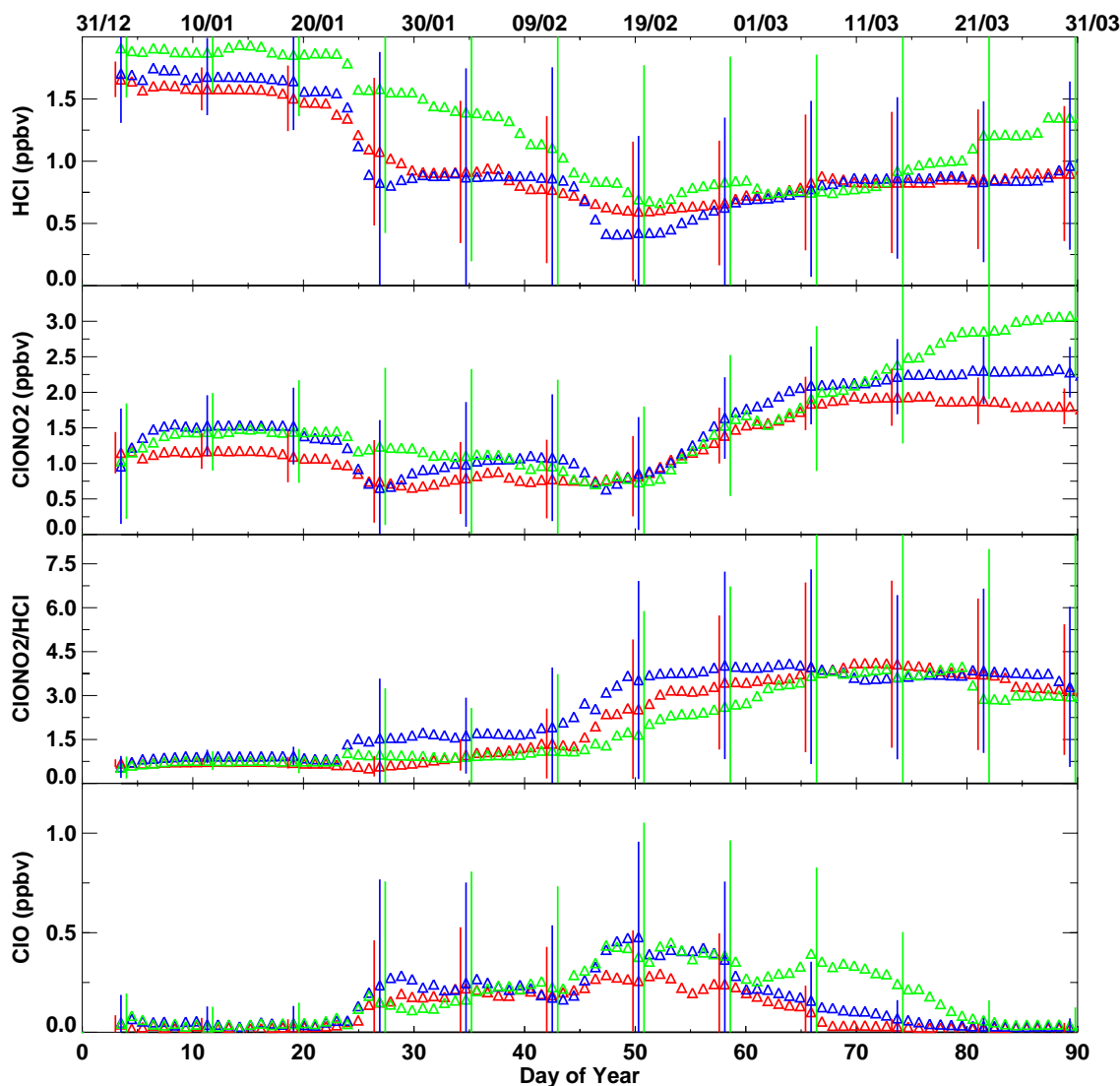
of NAT formation and NAT “rock” growth is lacking. The initial chemical concentrations were taken from the ACE-FTS measurement suite; those species which were not observed were taken from the CMAM model (e.g., de Grandpré et al., 2000).

Figure 5 shows one particular trajectory in this suite launched from an ACE measurement location on 9 January 2005. For this trajectory the HCl is not completely processed while the  $\text{ClONO}_2$  virtually disappears. Of the total amount of Cl, 2.1 ppbv, (and 60% HCl) about 1.9 ppbv is converted to  $\text{ClO}_x$  ( $\text{ClO}$  and  $\text{Cl}_2\text{O}_2$ ). The  $\text{ClO}_x$  disappears with a time constant of about 2 weeks and the main reservoir species formed is  $\text{ClONO}_2$ : HCl is much slower to reform. By the end of February, the trajectory  $\text{ClONO}_2/\text{HCl}$  ratio is about 4.3, somewhat higher than that for the measurements at that period. However, this ratio is trajectory (and also temperature) dependent. Other trajectories indicate the gradual processing of vortex air through the cold pool.

Figure 6 presents a composite of  $\text{ClONO}_2$ , HCl and their ratio from the set of vortex trapped trajectories initialized from 22.5, 23.5 and 24.5 km at the time of ACE occultations. For presentation, the values at each time have been averaged and at selected times the variance of the values have been plotted. The averaged values correspond to air parcels in a range of altitudes between 16 and 24.5 km, with values at later stages of the evolution tending to be at lower altitudes. The variability reflects the various situations that could have been measured by ACE-FTS and also the instability of the vortex, especially after mid February. The detailed trajectories indicate that not all encountered temperatures low enough for significant heterogeneous processing while others encountered extensive processing. This is also

evident from the plot in Fig. 6 taking into account the variability in the HCl which shows that HCl varies from very small values indicating rather complete processing to larger values which indicate little processing. Variability of measured HCl at 20.5 km is about 1.5 ppmv at the peak of the processing, similar to model variability at least for trajectories starting at 22.5 and 23.5 km. Similar results are observed for  $\text{ClONO}_2$ . However, the variability of the model is slightly larger than those of observations at 20.5 km (Fig. 1) in March because lower altitudes are considered by the model for this period. Figure 7 shows evolution of HCl,  $\text{ClONO}_2$  and their ratio inside the vortex between 12 and 30 km: variability of HCl is effectively larger for altitudes below 20 km in March. The larger variability of the model values may also result from the loss of identity of air parcels through mixing on a 60-day timescale (scale used for trajectory calculations). Where processing does occur, the depletion of  $\text{ClONO}_2$  is generally greater than that for HCl. The processing is clustered around late January and late February when the Arctic cold pool reaches its lowest temperatures as described above. Mean modeled values of HCl are about 1.5 ppbv until 25 January 2005 and show less processing than observed at 20.5 km (Fig. 1). This can be explained by the fact that the box model lacks representation of PSC types that occur in the first half of January. Modeled and observed HCl processing are similar: values close to zero, reflecting complete processing, are modeled even if the mean would show underestimation of processing in the model. The recovery of HCl during March leads to values ( $\sim 1$  ppmv) lower to those observed at 20.5 km (Fig. 1). Air sampled on the 50 hPa surface will capture parcels affected by heterogeneous chemistry during the peak processing period but at later stages will see unprocessed parcels from higher altitudes. Moreover, for this time period, the model is more representative of lower altitudes and thus to smaller values of HCl (Fig. 7). As discussed in Sect. 4,  $\text{ClONO}_2$  is highly variable during the pre-processing and the processing period. However,  $\text{ClONO}_2$  tends to be overestimated by the model during these periods. The modeled recovery starts after 20 February, while first signs of recovery were observed almost 10 days before by ACE.  $\text{ClONO}_2$  values reached during March (recovery phase) are in both cases (model and measurements) in good agreement, larger than 2 ppbv. The recovery of modeled HCl and  $\text{ClONO}_2$  starts simultaneously. On the contrary, a delay of almost 10 days is observed for HCl recovery from ACE measurements. The modeled  $\text{ClONO}_2/\text{HCl}$  ratio tends then to be smaller than the observed one until the beginning of March. After then, the ratio corresponds to altitudes lower than 20 km, where it is larger in both model and measurements. However, it is still slightly overestimated by the model.

The lowest panel in Fig. 6 shows the ClO that results from the processing. Bearing in mind the variability shown, the values are comparable with those of the measurements displayed in Fig. 5. However, we have not reproduced the ClO feature that is measured at about day 15. The box model



**Fig. 6.** Mean concentrations versus day of year for HCl (first panel),  $\text{ClONO}_2$  (second panel), HCl/ $\text{ClONO}_2$  ratio (third panel) and ClO (fourth panel) from vortex trapped trajectories. Colours represent different altitudes from which trajectories were initialized: 22.5 km (red), 23.5 km (blue) and 24.5 km (green). Error bars based on variance are shown at select times.

lacks representation of polar stratospheric cloud types that are not either ice or STS and temperatures below 191 K cover a large region in the first half of January 2005. The significant ClO values observed indicate that NAT processing was present.

## 6 Summary and conclusions

We have presented the first time series from space of the processing and recovery of the primary chlorine reservoirs HCl and  $\text{ClONO}_2$  in the Arctic polar vortex for the period January to March 2005 using the high resolution ACE-FTS. We also present average measurements for ClO during this period. The time evolution of HCl,  $\text{ClONO}_2$  and ClO as

well as the partitioning between the two reservoir molecules agrees well with previous observations and confirms our current understanding of chlorine activation during Arctic winter (Michelsen et al., 1999). Figure 7 presents a summary of the evolution of HCl,  $\text{ClONO}_2$  and of their ratio inside the Arctic vortex 2005. In early January the measurements (ClO in particular) indicate processing of the vortex air. The decrease in HCl and  $\text{ClONO}_2$  begins after 10 January. HCl vmrs stay very low until the end of February and HCl recovers slowly until 26 March. The first recovery of  $\text{ClONO}_2$  occurs between 9 February and the end of February and reaches a maximum between 2 and 10 March. Moreover, since the ACE-FTS samples a range of vortex latitudes during this period it also samples to what extent the vortex air

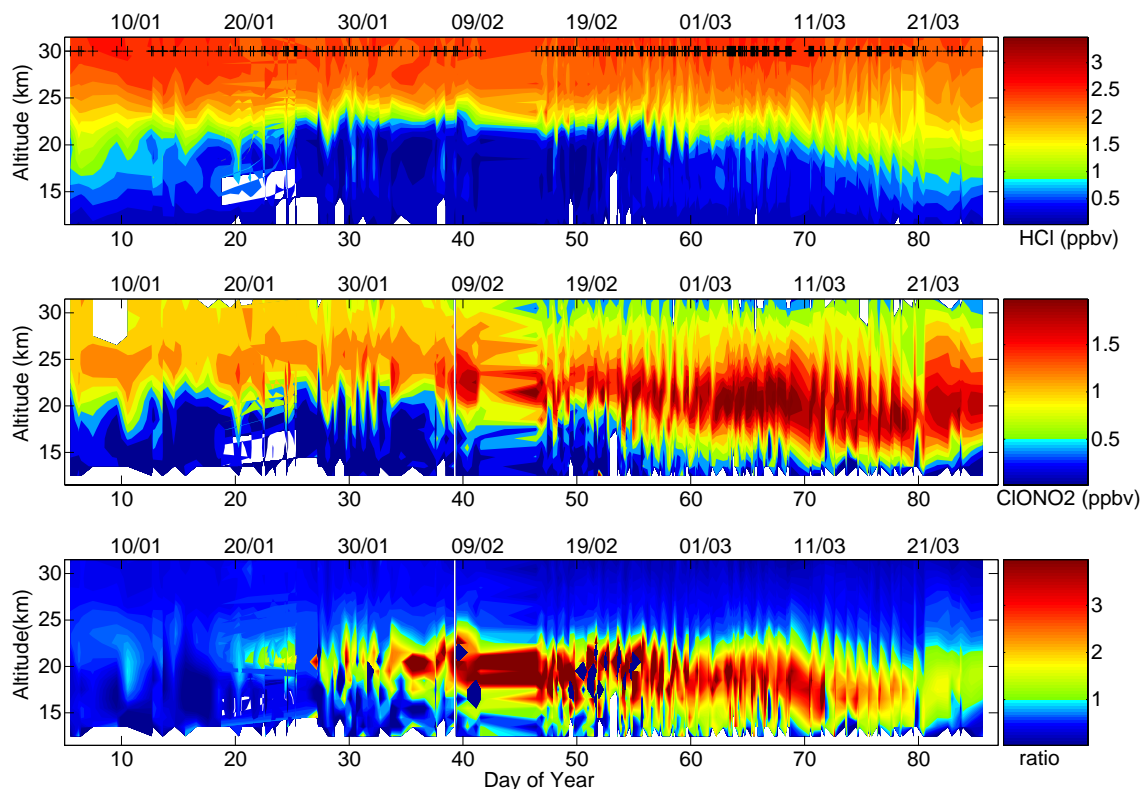


**Fig. 7.** Time series of the HCl (top), ClONO<sub>2</sub> (middle) and ClONO<sub>2</sub>/HCl (bottom) profiles measured by ACE-FTS between 10 and 31 km observed from 1 January 2005 to 26 March 2005 for measurements inside the vortex. Crosses on the top panel represent the actual measurement time. White areas correspond to missing data.

has been processed. Using a box model and measurements, the picture that emerges is consistent with our understanding of PSC processing. As vortex air is processed through the cold pool and circulates in the vortex, the chlorine reservoirs HCl and ClONO<sub>2</sub> are gradually converted to ClO<sub>x</sub>. The ACE-FTS thus samples air that is freshly processed with low HCl and ClONO<sub>2</sub> values and high ClO vmrs as well as air that has been partially processed and air which is beginning to recover pre-processing reservoir vmrs. Further analysis and comparison with measured ozone loss is in progress and should yield further insights to the 2005 Arctic ozone loss period.

*Acknowledgements.* Funding for ACE is provided by the Canadian Space Agency and the Natural Sciences and Engineering Research (NSERC) of Canada. Support was also provided by the NSERC-Bomem-CSA-MSI Industrial Research Chair in Fourier Transform Spectroscopy. Work at the Jet Propulsion Laboratory, California Institute of Technology was done under contract with the National Aeronautics and Space Administration. We thank S. McLeod and K. Gilbert for assistance.

Edited by: R. Volkamer

## References

- Bernath, P. F., McElroy, C. T., Abrams, M. C., Boone, C. D., Butler, M., Camy-Peyret, C., Carleer, M., Clerbaux, C., Coheur, P.-F., Colin, R., DeCola, P., DeMazière, M., Drummond, J. R., Dufour, D., Evans, W. F. J., Fast, H., Fussen, D., Gilbert, K., Jennings, D. E., Llewellyn, E. J., Lowe, R. P., Mahieu, E., McConnell, J. C., McHugh, M., McLeod, S. D., Michaud, R., Midwinter, C., Nassar, R., Nichitiu, F., Nowlan, C., Rinsland, C. P., Rochon, Y. J., Rowlands, N., Semeniuk, K., Simon, P., Skelton, R., Sloan, J. J., Soucy, M.-A., Strong, K., Tremblay, P., Turnbull, D., Walker, K. A., Walkty, I., Wardle, D. A., Wehrle, V., Zander, R., and Zou, J.: Atmospheric Chemistry Experiment (ACE): mission overview, *Geophys. Res. Lett.*, 32, L15S01, doi:10.1029/2005GL022386, 2005.
- Bonne, G. P., Stimpfle, R. M., Cohen, R. C., Voss, P. B., Perkins, K. K., Anderson, J. G., Salawitch, R. J., Elkins, J. W., Dutton, G. S., Jucks, K. W., and Toon, G. C.: An examination of the inorganic chlorine budget in the lower stratosphere, *J. Geophys. Res.*, 105(D2), 1957–1971, 2000.
- Boone, C. D., Nassar, R., Walker, W. A., Rochon, Y., McLeod, S. D., Rinsland, C. P., and Bernath, P. F.: Retrievals for the Atmospheric Chemistry Experiment Fourier Transform Spectrometer, *Appl. Opt.*, 44, 7218–7231, 2005.
- Bloom, S., da Silva, A., Dee, D., Bosilovich, M., Chern, J.-D., Pawson, S., Schubert, S., Sienkiewicz, M., Stajner, I., Tan, W.-W.,

- and Wu, M.-L.: The Goddard Earth Observing Data Assimilation System, GEOS DAS Version 4.0.3: Documentation and Validation, NASA, 104606 V26, 2005.
- Blumenstock, Th., Fischer, H., Friedle, A., Hase, F., and Thomas, P.: Column amounts of ClONO<sub>2</sub>, HCl, HNO<sub>3</sub> and HF from ground-based FTIR measurements made near Kiruna, Sweden, in late winter 1994, *J. Atmos. Chem.*, 26, 311–321, 1997.
- Carslaw, K. S., Luo, B., and Peter, Th.: An analytic expression for the composition of aqueous HNO<sub>3</sub>-H<sub>2</sub>SO<sub>4</sub> stratospheric aerosols including gas phase removal of HNO<sub>3</sub>, *Geophys. Res. Lett.*, 22, 1877–1880, 1995.
- Chartrand, D. J. and McConnell, J. C.: Evidence for HBr production due to minor channel branching at mid-latitudes, *Geophys. Res. Lett.*, 25, 55–58, 1998.
- Chipperfield, M. P., Santee, M. L., Froidevaux, L., Manney, G. L., Read, W. G., Waters, J. W., Roche, A. E., and Russell, J. M.: Analysis of UARS data in the southern polar vortex in September 1992 using a chemical transport model, *J. Geophys. Res.*, 101(D13), 18 861–18 881, 1996.
- Chipperfield, M. P., Lutman, E. R., Kettleborough, J. A., Pyle, J. A., and Roche, A. E.: Model studies of chlorine deactivation and formation of ClONO<sub>2</sub> collar in the Arctic polar vortex, *J. Geophys. Res.*, 102(D1), 1467–1478, 1997.
- De Grandpré, J., Beagley, S. R., Fomichev, V. I., Griffioen, E., McConnell, J. C., Medvedev, A. S., and Shepherd, T. G.: Ozone climatology using interactive chemistry: Results from the Canadian Middle Atmosphere Model, *J. Geophys. Res.*, 105, 26 475–26 492, 2000.
- Dessler, A. E., Conside, D. B., Morris, G. A., Schoeberl, M. R., Russell III, J. M., Roche, A. E., Kumer, J. B., Mergenthaler, J. L., Waters, J. W., Gille, J. C., and Yue, G. K.: Correlated observations of HCl and ClONO<sub>2</sub> from UARS and implications for stratospheric chlorine partitioning, *Geophys. Res. Lett.*, 22, 1721–1724, 1995.
- Douglass, A. R., Schoeberl, M. R., Stolarski, R. S., Waters, J. W., Russell III, J. M., Roche, A. E., and Massie, S. T.: Interhemispheric differences in springtime production of HCl and ClONO<sub>2</sub> in the polar vortices, *J. Geophys. Res.*, 100(D7), 13 967–13 978, 1995.
- Froidevaux, L., Livesey, N. J., Read, W. G., et al.: Early validation analyses of atmospheric profiles from EOS MLS on the Aura satellite, *IEEE Trans. Geosci. Remote Sensing*, 44(5), 1106–1121, 2006.
- Glatthor, N., von Clarmann, T., Fischer, H., Grabowski, U., Höpfner, M., Kellmann, S., Kiefer, M., Linden, A., Milz, M., Steck, T., Stiller, G. P., Mengistu Tsidu, G., Wang, D.-Y., and Funke, B.: Spaceborne ClO observations by the Michelson Interferometer for Passive Atmospheric Sounding (MIPAS) before and during the Antarctic major warming in September/October 2002, *J. Geophys. Res.*, 109, D11307, doi:10.1029/2003JD004440, 2004.
- Höpfner, M., von Clarmann, T., Fischer, H., Glatthor, N., Grabowski, U., Kellmann, S., Kiefer, M., Linden, A., Mengistu Tsidu, G., Milz, M., Steck, T., Stiller, G. P., and Wang, D. Y.: First spaceborne observations of Antarctic stratospheric ClONO<sub>2</sub> recovery: Austral spring 2002, *J. Geophys. Res.*, 109, D11308, doi:10.1029/2004JD004609, 2004.
- Jin, J. J., Semeniuk, K., Manney, G. L., Jonsson, A. I., Beagley, S. R., McConnell, J. C., Dufour, G., Nassar, R., Boone, C. D., Walker, K. A., Bernath, P. F., and Rinsland, C. P.: Severe Arctic ozone loss in the winter 2004/2005: observations from ACE-FTS, *Geophys. Res. Lett.*, in press, 2006.
- Kleinböhl, A., Bremer, H., Küllmann, H., Kuttippurath, J., Brownell, E. V., Canty, T., Salawitch, R., Toon, G. C., and Notholt, J.: Denitrification in the Arctic mid-winter 2004/2005 observed by airborne submillimeter radiometry, *Geophys. Res. Lett.*, 32, L19811, doi:10.1029/2005GL023408, 2005.
- Kistler, R., Collins, W., Saha, S., White, G., Woollen, J., Kalnay, E., Chelliah, M., Ebisuzaki, W., Kanamitsu, M., Kousky, V., van den Dool, H., Jenne, R., and Fiorino, M.: The NCEP-NCAR 50-year Reanalysis: Monthly Means CD-ROM and Documentation, *Bull. Amer. Meteorol. Soc.*, 82, 247–267, 2001.
- Mahieu, E., Zander, R., Duchatelet, P., Hannigan, J. W., Coffey, M. T., Mikuteit, S., Hase, F., Blumenstock, T., Wiacek, A., Strong, K., Taylor, J. R., Mittermeier, R., Fast, H., Boone, C. D., McLeod, S. D., Walker, K. A., Bernath, P. F., and Rinsland, C. P.: Comparisons between ACE-FTS and ground-based measurements of stratospheric HCl and ClONO<sub>2</sub> loadings at northern latitudes, *Geophys. Res. Lett.* 32, L15S08, doi:10.1029/2005GL022396, 2005.
- Manney, G. L., Sabutis, J. L., Pawson, S., Santee, M. L., Naujokat, B., Swinbank, R., Gelman, M. E., and Ebisuzaki, W.: Lower stratospheric temperature differences between meteorological analyses in two cold Arctic winters and their impact on polar processing studies, *J. Geophys. Res.*, 108(D5), 8328, doi:10.1029/2001JD001149, 2003.
- Manney, G. L., Livesey, N. J., Jimenez, C. J., Pumphrey, H. C., Santee, M. L., MacKenzie, I. A., and Waters, J. W.: EOS Microwave Limb Sounder observations of “frozen-in” anticyclonic air in Arctic summer, *Geophys. Res. Lett.*, 33, L06810, doi:10.1029/2005GL025418, 2006.
- Marti, J. and Mauersberger, K.: A survey and new measurements of ice vapor pressure at temperatures between 170 and 250 K, *Geophys. Res. Lett.*, 20, 363–366, 1993.
- Massie, S. T., Baumgardner, D., and Dye, J. E.: Estimation of polar stratospheric cloud volume and area densities from UARS, stratospheric aerosol measurement II, and polar ozone and aerosol measurement II extinction data, *J. Geophys. Res.*, 103(D5), 5773–5783, 1998.
- McHugh, M., Magill, B., Walker, K. A., Boone, C. D., Bernath, P. F., and Russell III, J. M.: Comparison of atmospheric retrievals from ACE and HALOE, *Geophys. Res. Lett.*, 32, L15S10, doi:10.1029/2005GL022403, 2005.
- Mellqvist, J., Galle, B., Blumenstock, T., Hase, F., Yashcov, D., Notholt, J., Sen, B., Blavier, J.-F., Toon, G. C., and Chipperfield, M. P.: Ground-based FTIR observations of chlorine activation and ozone depletion inside the Arctic vortex during the winter of 1999/2000, *J. Geophys. Res.*, 107(D20), 8263, doi:10.1029/2001JD001080, 2002.
- Michelsen, H. A., Salawitch, R. J., Gunson, M. R., Aellig, C., Kämpfer, N., Abbas, M. M., Abrams, M. C., Brown, T. L., Chang, A. Y., Goldman, A., Irion, F. W., Newchurch, M. J., Rinsland, C. P., Stiller, G. P., and Zander, R.: Stratospheric chlorine partitioning: Constraints from shuttle-borne measurements of [HCl], [ClNO<sub>3</sub>], and [ClO], *Geophys. Res. Lett.*, 23, 2361–2364, 1996.
- Michelsen, H. A., Webster, C. R., Manney, G. L., Scott, D. C., Margitan, J. J., May, R. D., Irion, F. W., Gunson, M. R., Russell III,

- J. M., and Spivakovsky, C. M.: Maintenance of high HCl/Cl<sub>y</sub> and NO<sub>x</sub>/NO<sub>y</sub> in the Antarctic vortex: A chemical signature of confinement during spring, *J. Geophys. Res.*, 104, 26 419, 1999.
- Müller, R., Peter, Th., Cruzten, P. J., Oelhaf, H., Adrian, G. P., von Clarmann, T., Wegner, A., Schmidt, U., and Lary, D.: Chlorine chemistry and the potential for ozone depletion in the Arctic stratosphere in the winter of 1991/1992, *Geophys. Res. Lett.*, 21, 1427–1430, 1994.
- Nassar, R., Bernath, P. F., Boone, C. D., Manney, G. L., McLeod, S. D., Rinsland, C. P., Skelton, R., and Walker, K. A.: ACE-FTS measurements across the edge of the winter 2004 Arctic vortex, *Geophys. Res. Lett.*, 32, L15S05, doi:10.1029/2005GL022671, 2005.
- Payan, S., Camy-Peyret, C., Jeseck, P., Hawat, T., Durry, G., and Lefèvre, F.: First direct simultaneous HCl and ClONO<sub>2</sub> profile measurements in the Arctic vortex, *Geophys. Res. Lett.*, 25, 2663–2666, 1998.
- Rinsland, C. P., Gunson, M. R., Abrams, M. C., Lowes, L. L., Zander, R., Mahieu, E., Goldman, A., and Irion, F. W.: April 1993 Arctic profiles of stratospheric HCl, ClONO<sub>2</sub> and CCl<sub>2</sub>F<sub>2</sub> from atmospheric trace molecule spectroscopy/ATLAS 2 infrared solar occultation spectra, *J. Geophys. Res.*, 100(D7), 14 019–14 027, 1995.
- Rothman, L. S., Jacquemart, D., Barbe, A., Benner, D. C., Birk, M., Brown, L. R., Carleer, M. R., Chackerian Jr., C., Chance, K., Coudert, L. H., Dana, D., Devi, V. M., Flaud, J.-M., Gamache, R. R., Goldman, A., Hartmann, J.-M., Jucks, K. W., Maki, A. G., Mandin, J.-M., Massie, S. T., Orphal, J., Perrin, A., Rinsland, C. P., Smith, M. A. H., Tennyson, J., Tolchenov, R. N., Toth, R. A., Vander Auwera, J., Varanasi, P., and Wagner, G.: The HITRAN 2004 molecular spectroscopic database, *J. Quant. Spectrosc. Radiat. Trans.*, 96, 139–204, 2005.
- Santee, M. L., Froidevaux, L., Manney, G. L., Read, W. G., Waters, J. W., Chipperfield, M. P., Roche, A. E., Kumer, J. B., Mergenthaler, J. L., and Russell III, J. M.: Chlorine deactivation in the lower stratospheric polar regions during late winter: Results from UARS, *J. Geophys. Res.*, 101(D13), 18 835–18 859, 1996.
- Santee, M. L., Manney, G. L., Waters, J. W., and Livesey, N. J.: Variations and climatology of ClO in the polar lower stratosphere from UARS Microwave Limb Sounder measurements, *J. Geophys. Res.*, 108(D15), 4454, doi:10.1029/2002JD003335, 2003.
- Solomon, P., Barrett, J., Connor, B., Zoonematkermani, S., Parrish, A., Lee, A., Pyle, J., and Chipperfield, M.: Seasonal observations of chlorine monoxide in the stratosphere over Antarctica during the 1996–1998 ozone holes and comparison with the SLIMCAT three-dimensional model, *J. Geophys. Res.*, 105(D23), 28 979–29 001, 2000.
- Stachnik, R. A., Salawitch, R., Engel, A., and Schmidt, U.: Measurements of chlorine partitioning in the winter Arctic stratosphere, *Geophys. Res. Lett.*, 26, 3093–3096, 1999.
- Stimpfle, R. M., Cohen, R. C., Bonne, G. P., Voss, P. B., Perkins, K. K., Koch, L. C., Anderson, J. G., Salawitch, R. J., Lloyd, S. A., Gao, R. S., Del Negro, L. A., Keim, E. R., and Bui, T. P.: The coupling of ClONO<sub>2</sub>, ClO, and NO<sub>2</sub> in the lower stratosphere in-situ observations using the NASA-ER2 aircraft, *J. Geophys. Res.*, 104(D21), 26 705–26 714, 1999.
- Webster, C. R., May, R. D., Toohey, D. W., Avallone, L. M., Anderson, J. G., Newman, P., Lait, L., Schoeberl, M. R., Elkins, J. W., and Chan, K. R.: Chlorine chemistry on polar stratospheric cloud particles in the Arctic winter, *Science*, 261, 1130–1133, 1993.
- WMO (World Meteorological Organization): Scientific Assessment of Ozone Depletion: 2002, Global Research and Monitoring Project – Report No. 47, Geneva, 2003.